

Comparison between SOLPS-ITER and B2.5-Eunomia for simulating Magnum-PSI

J. Gonzalez¹, R. Chandra^{1,2}, H. J. de Blank¹, E. Westerhof¹

¹ DIFFER, de Zaale 20, 5612AJ, Eindhoven, The Netherlands

² Department of Applied Physics, Aalto University, Espoo, Finland

E-mail: j.gonzalezmunos@differ.nl

Abstract. The interaction among plasma, neutrals and surfaces in fusion reactors is of immense importance for heat and particle control, specially for the next generation of devices. Heat loads of 10 MWm^{-2} are expected for steady state operation at ITER and up to 20 MWm^{-2} in slow transient situations. To study the complex physics appearing between the plasma and the divertor material, as well as techniques for heat flux mitigation, plasma linear devices are employed. Magnum-PSI, located at DIFFER, can reproduce heat and particle loads expected at ITER. However, due to the complexity of the plasma-wall interaction, numerical models are required to better understand the experiments and to extrapolate the results to a tokamak divertor configuration. For tokamak geometries, SOLPS-ITER (formerly known as B2.5-Eirene) is employed to solve the plasma and neutral distribution in a coupled way. However, the utilization of this code for linear devices is not straight forward. Thus, a neutral module was developed with linear devices in mind, named Eunomia. Nevertheless, there is still a relevant interest in using SOLPS-ITER with linear devices, as it allows to easily transfer knowledge about relevant atomic and molecular processes close to the surface and the effect of different mitigation techniques. This work presents a systematic comparison between the two neutral modules, Eirene and Eunomia, in stand-alone and coupled runs. Special attention is paid to the implementation of plasma-neutral interactions, in which both codes diverge significantly. The sources of particles and energy that are used by B2.5 in a coupled run are analysed. Significant differences in the implementation of electron impact ionization, molecular assisted recombination and proton-molecule elastic collisions lead to disparate sources of particles and energy and, in some cases, differences in the distribution of neutrals achieved by each code. Moreover, a double counting in proton-atom collisions was identified in Eunomia as a result of this analysis, artificially increasing the plasma-neutral sink of energy. These would lead to different plasma evolutions in coupled runs. Nevertheless, additional free parameters in both coupled code suites leave sufficient freedom to match experimental data. Additional data would be required to further constrain these parameters and the coupled solution.

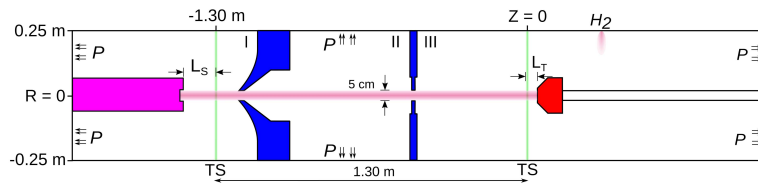


Figure 1: Simplified geometry section of Magnum-PSI. The three chambers source (I), beam dump (II) and target (III) are separated by skimmers marked in solid blue. The target position, marked in red, can be axially transposed. Figure taken with permission from Ref. [7] with slight modifications.

1. Introduction

The high energy obtained from the fusion of light species produced in the core of a tokamak is redirected towards the vessel divertor. This surface needs to endure heat loads that for ITER [1] will go from 10 MWm^{-2} in steady state operation up to 20 MWm^{-2} during slow transients [2]. The high fluxes of heat and particles need to be reduced and removed to extend the lifetime of the divertor walls. Thus, the interaction of the high energy plasma, the neutrals present inside the vessel (from recombination, sputtering and gas puffing) and the wall material is of immense importance for the next generation of fusion devices.

To study the complex interaction between plasma and target as well as the basic principles of heat and particle fluxes mitigation, devices like Magnum-PSI [3] are employed. This plasma linear device can generate similar conditions to those expected to be achieved at ITER's divertor targets, reaching hydrogen flux densities of $10^{23} - 10^{25} \text{ m}^{-2}\text{s}^{-1}$ with electron and ion temperatures of $1 - 5 \text{ eV}$ [4]. The basic geometry of Magnum-PSI, in the cases presented in this work, is shown in Fig. 1. Magnum-PSI is divided into three chambers separated by skimmers: source, beam dump and target, marked as I, II and III respectively. These skimmers limit the diameter of the plasma beam to around 5 cm. Moreover, the magnetic field must be large enough so the plasma beam is not too wide, which would result in an extreme head load on the first skimmer. The pressure is maintained at a specific level in each chamber thanks to the cryogenic pumps marked with P . Particularly relevant is the pressure in the target chamber, which is kept low to match conditions near the divertor. In the target chamber, a test material, usually tungsten, is exposed to the plasma beam. A gas puff can be injected into the target chamber to simulate detachment by increasing the chamber pressure. Different diagnostics are applied during a typical operation of Magnum-PSI, including Thomson Scattering near the target [5]. In a typical Magnum-PSI run, a Hydrogen plasma is generated at the source chamber by a cascaded arc source [6].

Due to the involved problem that is the plasma-surface interaction in Magnum-PSI, numerical models are required to better understand the experimental data and to validate numerical modelling against experiments in relevant regimes for divertor detachment in order to provide a predictive model capability for reactor divertor

modelling and design. Two numerical codes are currently being used to model Magnum-PSI in a wide range of scenarios: SOLPS-ITER, formerly known as B2.5-Eirene, [8, 9] and B2.5-Eunomia [10]. Both codes use the same fluid plasma solver, B2.5, and a Monte-Carlo code, Eirene [11, 12] and Eunomia respectively, to solve the neutral distribution. An important effort has been done in developing B2.5-Eunomia and validating it against experiments [7]. However, the distinct geometry and configuration compared to a classical tokamak make it a challenge for simulation with SOLPS-ITER, as previous simulations of linear devices have shown [13, 14, 15].

As SOLPS-ITER is widely used in the fusion community, it is reasonable to use it in the modelling of Magnum-PSI to easily extrapolate the relevant atomic and molecular (A&M) processes near the target to a divertor configuration. Thus, an effort is currently being done to perform simulations of Magnum-PSI using SOLPS-ITER. This will ease the analysis of Magnum-PSI experiments aimed to recreate ITER divertor like conditions and will allow to extract relevant information of plasma-surface interaction in fusion devices. But firstly, a comparison between the two neutral codes needs to be carried out, to ensure that the implementation of plasma-neutral interactions in SOLPS-ITER is capable to reproduce the B2.5-Eunomia cases that have been previously compared with experiments [7, 16]. Good agreement between simulations and experiments was found for a high and low density case and a wide range of pressure, although discrepancies between the two still appeared, particularly in the plasma density.

This work deals with a systematic comparison of the two neutral gas modules currently being used to simulate Magnum-PSI: Eirene and Eunomia. The standard set of collision processes used in each code for H plasma are analysed here. For Eunomia, these collisions are the ones used in Ref. [7]. For Eirene, the reactions obtained while generating a generic case for a tokamak in SOLPS-ITER for H and H₂ are employed. However, modifications to both codes via input files or small changes in the code are applied to match as much as possible the physics inside Eirene and Eunomia. Section 2 presents the basic differences and similarities between Eirene and Eunomia and the modifications that have been performed to allow the comparison between the two codes. Then, Sec. 3 introduces a case without collisions used to check that both codes implement the same sources of neutral particles. The effects of different plasma-neutral collision processes and how they are implemented are presented in Sec. 4 using a frozen plasma background extracted from the High Density scenario from Ref. [7]. Differences in elastic proton-atom and proton-molecule collisions, as well as electron impact ionization and molecular assisted recombination, are studied in detail. Finally, conclusions are presented in Sec. 5.

2. Differences and similarities between Eirene and Eunomia

As the plasma solution in both codes analysed here derive from the same fluid plasma module (B2.5), it is expected that the main differences appear from the neutral solution provided by either Eirene or Eunomia. However, as the two modules are coupled with

the plasma solution and evolve in conjunction during the iterative process, differences in the sources of particles and energy for B2.5 would result in different plasma distributions. Thus, it is important to analyse the disagreements between the two neutral solutions independently from the plasma evolution.

For this purpose, a case in which the plasma solution is in a frozen state (not evolving) during the iterative process is used to study the differences between the two neutral modules. The plasma background from the High Density case presented in Ref. [7] is used for all the cases shown in this work. This plasma regime reproduces the expected particle and heat flux in the ITER divertor. The effect of these differences in coupled runs, accounting for plasma evolution, is reserved for a follow up paper.

The main differences that have an impact on the distribution of neutrals arise from wall reflection models and collision processes. These differences in the implementation of plasma-neutral collision processes are analysed in Sec. 4. In the standard Eirene wall model [9], an atom not being absorbed by the wall and experiencing a reflection has two possible outcomes: either it is reflected keeping its velocity, just changing its direction, or it is reintroduced as a molecule or atom with a thermal distribution based on the wall temperature. These options are controlled via the Eirene input file, adjusting probabilities for each event. To carry out this comparison, some modifications have been performed to both codes to match as much as possible the sources of neutral particles. A user defined model for wall reflection in Eirene has been implemented. This model is equivalent to Eunomia's, in which an incident H atom has a fixed probability to be reflected as a thermal atom, at wall temperature, or it is reflected as a H₂ molecule, also at wall temperature. These assumed probabilities can be set by the user and for Magnum-PSI they were adjusted to match experimental results [10].

Although individual vibrational states can be traced in Eunomia, this functionality has been disabled to better match a standard Eirene run. Even when Eirene should be able of the same individual tracking [17], their effect is out of the scope of this work as Eirene is typically used without this capability.

Regarding target recycling, the main difference between the two neutral codes is the sampling of angle and energy distributions. Although both assume cosine-Maxwellian distribution, the speed of the recycled particle is computed differently in Eirene as the TRIM reflection database is used to get the reflected neutral velocity. For this comparison, TRIM model has been disabled to have a sampling process as close as possible to Eunomia's.

Even though it is not possible to use the same neutral mesh in both codes, the plasma grid, based on B2.5, has been set identically in both code suites. Nevertheless, the two neutral grids have been generated to have similar cell sizes and the exact same contour, meaning that the exact matching outside the plasma regions is not necessary as both meshes are equivalent.

3. Reference case

A reference case, in which no collisional processes are included, is presented here. This case includes four sources of neutral particles: one is the target recycling, two from the plasma source (one parallel to the plasma beam and another one perpendicular), and a final source for volume recombination.

The aim of this case is twofold: first, to check that all sources and wall models produce similar effects in the simulation, and to present a reference case for the study of collision processes in Sec. 4.

The tungsten target has a 100% recycling of incident ions, in a ratio of 0.9 H^+ into H and 0.1 H^+ into H_2 . Some differences between Eirene and Eunomia still remain, *e.g.*, in sampling of particles from target recycling. In Eirene, a particle is sampled from the plasma influx and it is then accelerated as it passes the non-calculated Debye sheath. In Eunomia, a neutral particle is directly sampled from the local plasma influx at the sheath. However, these differences do not significantly impact the final distribution of neutrals in the Magnum-PSI vacuum chamber. The remaining vessel walls are assumed to be stainless steel and to have a 90% reflection of incident H into thermal H , at wall temperature of 300 K and 10% into thermal H_2 , at the same temperature.

The neutrals from the plasma source come from un-ionized H_2 molecules dissociated by the cascaded-arc source, as Magnum-PSI requires huge gas flows, between 4 – 8 slm to obtain the desired plasma densities.

Volumetric recombination is included in both codes as it is treated as a source of neutrals from the plasma region. This process is mostly computed from the plasma side, and the neutral module only samples the new neutral particles. No significant difference has been found in the sampling of particles from volumetric recombination.

The feedback loops that maintain the chamber pressures at a specific value have been disabled. The surfaces corresponding to the pumps have been set with a 10% probability of pumping incident atoms or molecules. The probability of absorption when the pressure feedback loop is active remains close to the imposed value in both codes, meaning that a pressure dependent absorption probability has very little influence for the cases presented here.

The distribution of H and H_2 in the complete Magnum-PSI vessel can be found in figures 2 and 3, respectively. A large concentration of H and H_2 appears near the regions of particle sources: plasma source and target recycling. The absence of collision processes results in almost no gradients in temperature or density. High temperature and density appear at the source of neutrals, as H from the source is injected at 3000 K and atoms from the target recycling have even higher temperature. However, a particle coming from any of these high temperature sources will rapidly interact with a wall and continue as a lower energy (300 K) particle until it is pumped away. In this reference case, walls are the only mechanism of thermalizing neutrals as collisions with the plasma are disabled and no source of ions appears due to ionization.

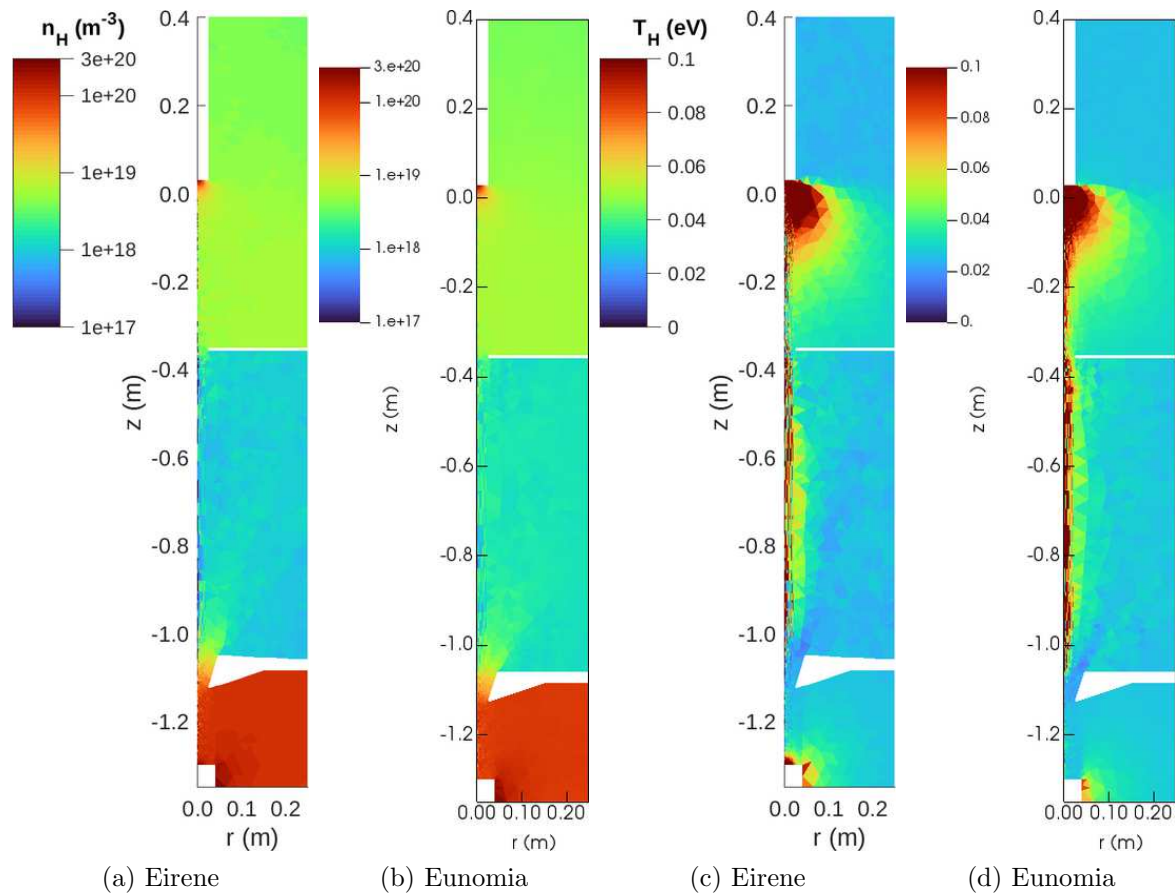


Figure 2: Density (left) and temperature (right) distribution of atomic Hydrogen in reference case for Eirene and Eunomia. The plasma beam expands just a few centimetres from the axis. The plasma source is located at -1.3m and the target at 3cm in the axial direction.

4. The effect of collision processes

As stated above the main differences between the two neutral codes, not solvable by input file modifications or small code changes, come from the different implementation of plasma-neutral collisions. This section analyses in detail the effect of the different implementation of collision processes.

The only plasma-neutral process not included in this comparison is the dissociation of molecules by electron impact, see Tab. 1 with a constant electron energy loss per collision of 10.5eV . This process produce similar sink of electron energy (Tab. 2) and neutral profiles (Fig. 4). Small differences still appear due to statistical differences, particularly for the low temperature of H_2 achieved.

4.1. Elastic $p + H$

The standard approaches of Eirene and Eunomia dealing with proton and H interactions are presented in table 8. Eirene only includes CX, using the cross-section information

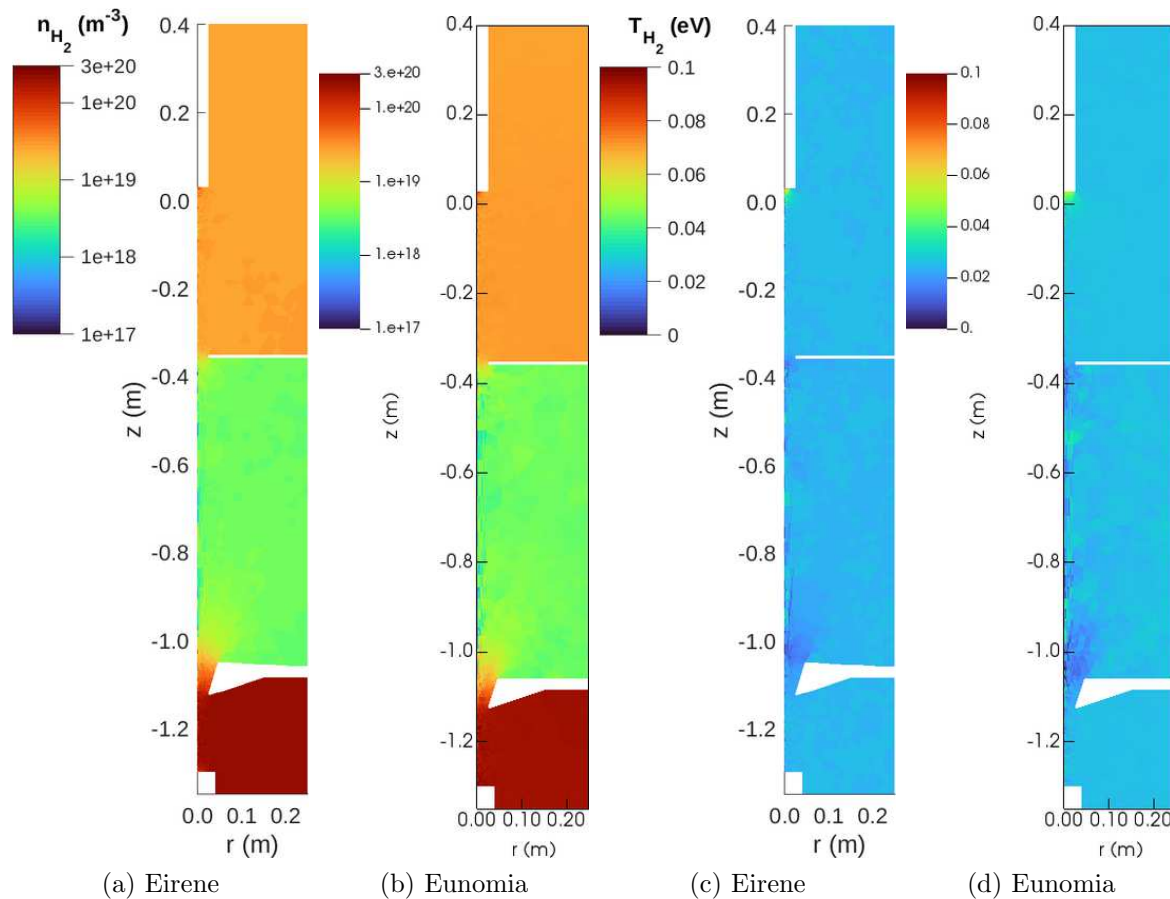


Figure 3: Density (left) and temperature (right) distribution of molecular Hydrogen in reference case for Eirene and Eunomia. The plasma beam expands just a few centimetres from the axis. The plasma source is located at -1.3m and the target at 3cm in the axial direction.

	Type	Formula	Database
Eirene	DS	$e + \text{H}_2 \longrightarrow \text{H} + \text{H} + e$	AMJUEL 2.2.5
Eunomia			

Table 1: Dissociation (DS) reaction employed in the two neutral modules. Energy losses per collision are constant to 10.5eV in both codes.

Case	Electron Energy (W)
Eirene	-430
Eunomia	-380

Table 2: Total electron energy source for the case of DS interaction. Both codes produce a similar sink of electron energy with a small difference (of 50W) related with statistical noise.

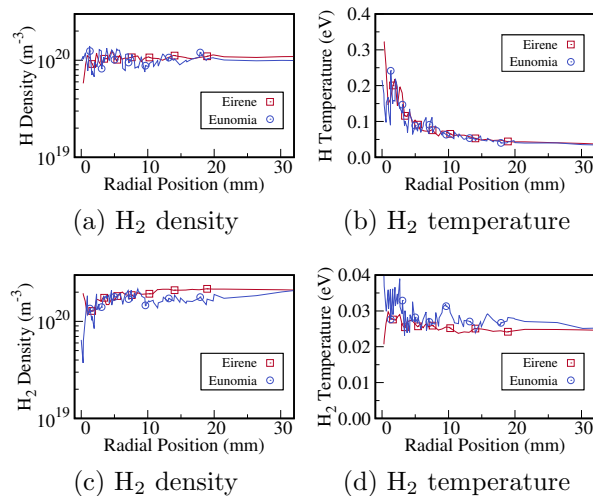


Figure 4: Radial profile of density (left) and temperature (right) of H (top row) and H₂ (bottom row) at $z = -1.2$ m. Only DS elastic collision is included in the simulation. Similar profiles are found between the two neutral modules with only small statistical errors.

	Type	Formula	Database
Eirene	CX	$p + H \longrightarrow H + p$	HYDHEL 3.1.8
Eunomia	CX	$p + H \longrightarrow H + p$	HYDHEL 3.1.8
	EL	$p + H \longrightarrow p + H$	AMJUEL 0.1T

Table 3: Reactions used by Eirene and Eunomia to implement $p + H$ collisions. CX stands for charge-exchange and EL refers to elastic collision.

from HYDHEL 3.1.8 and assuming an exchange of identity (backwards scattering) [18] which produces a factor two, thus not requiring to account for the classical elastic reaction [19]. Eunomia implements a purely backward scattering for the charge-exchange processes, but adds an isotropic elastic exchange [20]. This is incorrect and the elastic collision, with the current implementation of CX, should not be employed as it will lead to double counting. Thus, it is important to study the effect of this erroneous implementation and also to check if both codes produce similar results when only backwards scattering is accounted for. An erratum is being prepared to address the impact of this issue in previous published coupled runs, as those in Ref. [7, 16].

Figure 5 presents the radial profiles of atomic Hydrogen at $z = -1.2$ m, a midpoint in the source chamber for three cases: Eirene (using only CX), Eunomia using CX and EL and Eunomia using only CX. All the cases presented here provide similar profiles in both, density and temperature up to Monte-Carlo noise level.

Nevertheless, even with similar neutral distributions, the energy exchange with the plasma varies. Table 4 presents the ion energy sink for the three cases described above. Both, Eirene and Eunomia using a backward scattering for CX produce the same source

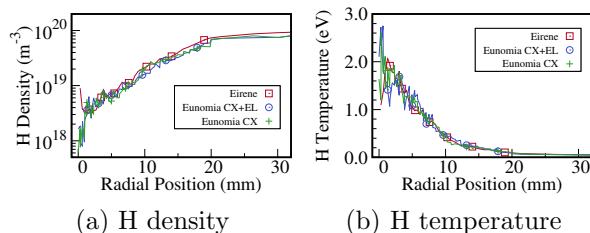


Figure 5: Radial profile of density (left) and temperature (right) of H at $z = -1.2$ m. In Eirene, only charge-exchange is accounted for. Eunomia can include CX and EL collisions.

Case	Ion Energy (W)
Eirene	-479
Eunomia CX+EL	-542
Eunomia CX	-461

Table 4: Total ion energy source for the case of $p + \text{H}$ EL interaction. The addition of EL process in Eunomia increases the energy exchanged between plasma and neutrals.

of energy for the ions, while incorrectly accounting for forward scattering in Eunomia, the EL process, increases the ion energy sink calculated by almost 100 W.

4.2. Elastic $p + \text{H}_2$

The main difference in the implementation of $p + \text{H}_2$ elastic exchange comes from the calculation of the anisotropic scattering angle. Eunomia uses the scattering angle introduced in Ref. [21] and later extended to molecules in Ref. [22]. In these references, the anisotropic angle is calculated as:

$$\cos \theta = \frac{2 + \alpha E_r - 2(1 + \alpha E_r)^R}{\alpha E_r} \quad (1)$$

where R is a random number between $[0, 1)$, E_r is the relative energy between the two colliding species and α is a collision dependent parameter. For the particular case of $p + \text{H}_2$ elastic collisions, $\alpha = 10^6$ [22]. On the other hand, Eirene uses the generalized Morse potential described in Ref. [19].

This difference in implementation leads to quite disparate results, as presented in Fig. 6. Distributions of H_2 in the plasma region (where collisions take place) present a factor 2 of difference between the two codes. This will also affect processes in which a H_2 molecule is involved (as MAR, neutral-neutral collisions or dissociation) as different profiles could lead to different rates and/or distribution of neutrals and plasma. Moreover, there is a significant difference of ~ 100 W in the energy sink of for ions between the two codes, as presented in table 5. Thus, Eunomia extracts more energy from the plasma ions than Eirene via EL collisions with molecules.

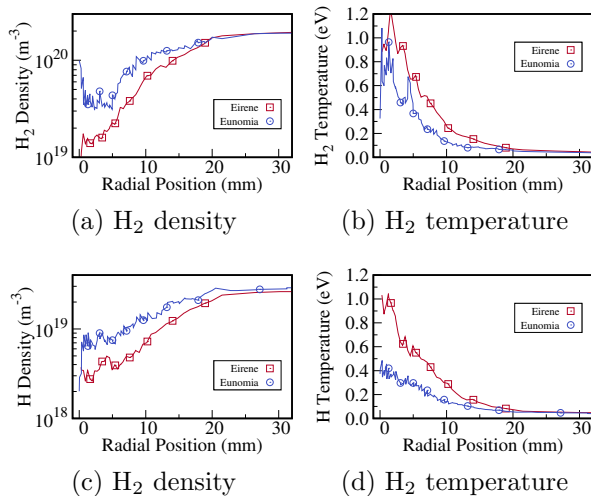


Figure 6: Radial profile of density (left) and temperature (right) of H_2 at $z = -1.2$ m (top row) and $z = 0.0$ m (bottom row). Only $p + \text{H}_2$ elastic collision is included in the simulation. This leads to significant difference between the results from Eirene and Eunomia at plasma beam region ($r < 0.02$ m).

Case	Ion Energy (W)
Eirene	-370
Eunomia	-490

Table 5: Integrated sources for ion energy for the case of $p + \text{H}_2$ EL interaction.

4.3. MAR

Molecular Assisted Recombination (MAR) is of huge importance [16] to understand molecule-plasma interaction in Magnum-PSI. This occurs when a proton exchanges charge with a H_2 molecule and then a free electron dissociates the charged molecule, resulting in three H atoms. This process is usually dealt with in a two-step implementation. However, both neutral codes deal with the second step, dissociation of H_2 , quite differently.

Table 6 shows the two step process of Molecular Assisted Recombination. Eunomia assumes that the dissociation of the H_2^+ particle results in a excited H-atom and a ground level H-atom. The excited particle is then either ionized or de-excited with a probability linked to the Einstein coefficient for photon emission. On the other hand, Eirene has a more involved approach for these processes. After the CX occurs, the impacting electron with the H_2^+ molecular ion will result in three possibilities: 1) two neutral H atoms, 2) one H atom and one H ion or 3) two H ions. These processes are read from AMJUEL 2.2.14, 2.2.12 and 2.2.11 respectively. Moreover, Eirene reads the energy loss by the impacting electron of process 2.2.14 from H.8 of AMJUEL database, which highly affect the energy rate per process. These distinct implementations lead to quite different sources of ion particles, energy and electron source energy calculated by

	Type	Formula	Database
Eirene	CX	$p + H_2 \longrightarrow H + H_2^+$	AMJUEL 3.2.3
	DS	$e + H_2^+ \longrightarrow H^+ + H^+ + 2e$	AMJUEL 2.2.11
	DS	$e + H_2^+ \longrightarrow H + H^+ + e$	AMJUEL 2.2.12
	DS	$e + H_2^+ \longrightarrow H + H$	AMJUEL 2.2.14
Eunomia	CX	$p + H_2 \longrightarrow H + H_2^+$	AMJUEL 3.2.3
	DS	$e + H_2^+ \longrightarrow H + H^*$	Spontaneous
		$H^* \longrightarrow \begin{cases} H^+ + e \\ H + h\nu \end{cases}$	Spontaneous

Table 6: Reactions used by Eirene and Eunomia to implement MAR. CX stands for charge exchange and DS refers to dissociation.

	Eirene	Eunomia
Electron Energy (W)	-1427	-457
Ion Energy (W)	191	-553
Ion particle (part/s)	-1.3e20	-2.9e20

Table 7: Integrated sources for electron energy, ion energy and ion particles when MAR is used alone in Eirene and Eunomia. These values exclude recombination.

the neutral code, which will be passed back to B2.5.

Table 7 summarizes the main sources of energy and particles calculated by Eirene and Eunomia when MAR is used. Large differences in the energy sources appear. In particular, the ion energy source becomes positive in Eirene as a result of the balance between the energy loss due to CX with molecules and the generation of new ions in the dissociation processes. Thus, the balance between ions disappearing from the simulation due to CX and new ions being generated in the dissociation process differs in both codes.

However, these different implementations result in quite similar neutral distributions when applied to an Eirene/Eunomia stand-alone case, as Fig. 7 shows. Only small differences in the radial profiles arise, particularly in the temperature profile of figures 7d and 7b.

4.4. Electron Impact Ionization/Excitation

The treatment of inelastic collisions between electrons and H atoms is implemented in a different way in typical operation of Eirene and Eunomia. Eunomia uses HYDHEL processes for ionization (2.1.5) and excitation (2.1.1), in which excited atoms can then later be ionized or de-excited back to ground state. The energy loss of the electron involved in the collision process is fixed at -13.6 eV for ionization and -10.2 eV for excitation to the first state. As shown in Tab. 8, in Eunomia the excited atom is then de-excited and the energy is lost due to radiation or it suffers a spontaneous ionization.

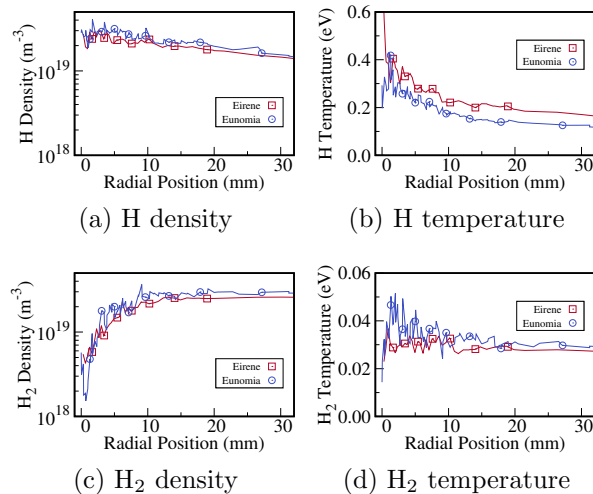


Figure 7: Radial profile of density (left) and temperature (right) at $z = 0.0$ m for atomic H (top row) and molecular H (bottom row). MAR is the only active process.

	Type	Formula	Database
Eirene	EI	$e + H \longrightarrow e + H^+ + e$	AMJUEL 2.1.5
Eunomia	EI	$e + H \longrightarrow e + H^+ + e$	HYDHEL 2.1.5
	EX	$e + H \longrightarrow e + H^*$	HYDHEL 2.1.1
		$H^* \longrightarrow \begin{cases} H^+ + e \\ H + h\nu \end{cases}$	Spontaneous

Table 8: Reactions used by Eirene and Eunomia to implement electron impact ionization. EI stands for ionization and EX refers to excitation.

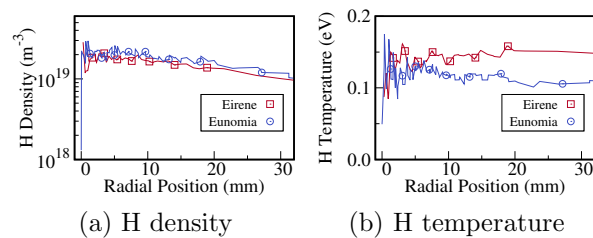


Figure 8: Radial profile of density (left) and temperature (right) at $z = 0.0$ m for atomic H. Eirene uses AMJUEL with a variable energy loss for electrons to account for an effective ionization rate. Eunomia uses HYDHEL for EI and EX with a constant loss per ionization.

Eirene reads an effective ionization rate from AMJUEL H.4 2.1.5 process which accounts for excitation and subsequent ionization as well. The associated electron energy losses is obtained from the AMJUEL database as well (H.10 2.1.5).

These processes being treated quite differently in the two neutral modules result in quite similar radial profiles in the TS target position, as shown in Fig. 8. However,

	Eirene	Eunomia
Electron Energy (W)	-589	-193
Ion particle (part/s)	1.3e19	1.9e19

Table 9: Integrated sources for electron energy and ion particles when electron impact ionization and excitation is used alone in Eirene and Eunomia. These values exclude recombination.

the resulting sources are completely different. Table 9 summarizes the electron energy and ion energy source when using the approach defined above for electron H inelastic collisions. Although while the amount of new ions calculated in both codes is quite similar, the energy sink of electrons is much larger in Eirene than in Eunomia. This indicates that the constant energy loss approach taken by Eunomia is not equivalent to the effective rate used in Eirene, at least for this particular scenario of Magnum-PSI.

5. Conclusions

Comparison of two numerical codes is always an intricate task, as different implementation of similar physical processes can result in quite different outputs. Nevertheless, this is now required as simulations for Magnum-PSI are switching from the dedicated neutral gas module Eunomia to the widely used Eirene module, part of SOLPS-ITER. The different implementation of plasma-neutral interactions results in a quite different energy exchange and neutral distributions.

This work does not take into account other interesting capabilities of Eunomia, as tracing individual vibrational states, which could become of importance in the simulation of Magnum-PSI and fusion devices. Thus, this should be addressed in a future work after these capabilities have been ported from Eunomia to Eirene.

In Eunomia more energy is extracted from the plasma ions, particularly due to MAR and $p + H_2$ elastic collisions. Moreover, a double counting of $p + H$ interactions in Eunomia was identified, whose impact in coupled runs will be addressed in an erratum for Ref. [7, 16]. In Magnum-PSI simulations, Ohmic heating in the plasma beam is directly controlled by the electric potential at the source, which is unknown and it is manually adjusted to match experimental data at the TS target position [7]. Thus, the lower ion energy sink calculated by Eirene will result in a completely different value of this free parameter to obtain similar plasma temperatures in the target chamber. The different implementation of collision processes between Eirene and Eunomia has an impact on the plasma evolution, which will be shown in a future comparison with coupled runs of Eirene and Eunomia with the CFD plasma code B2.5.

Measurements of the distributions of neutrals in the plasma beam would provide valuable information to compare with the disparate neutral distributions obtained by Eirene and Eunomia. These data will aid in identifying which neutral module produces results closer to experiments. This will determine if additional functionalities from

Eunomia, *i.e.* the capability to trace individual vibrational states, are needed in Eirene to properly simulate Magnum-PSI.

Acknowledgments

This work has been carried out within the framework of the EUROfusion Consortium, funded by the European Union via the Euratom Research and Training Programme (Grant Agreement No 101052200 — EUROfusion). Views and opinions expressed are however those of the author(s) only and do not necessarily reflect those of the European Union or the European Commission. Neither the European Union nor the European Commission can be held responsible for them. This work was carried out on the Dutch national e-infrastructure with the support of SURF Cooperative and the EUROfusion High Performance Computer Marconi-Fusion hosted at Cineca (Bologna, Italy). This work is part of the research programme "The Leidenfrost divertor: a lithium vapour shield for extreme heat loads to fusion reactor walls" with project number VI.Vidi.198.018, which is (partly) financed by NWO.

- [1] H Bolt, V Barabash, G Federici, J Linke, A Loarte, J Roth, and K Sato. Plasma facing and high heat flux materials—needs for ITER and beyond. *Journal of Nuclear Materials*, 307:43–52, 2002.
- [2] JP Gunn, S Carpentier-Chouchana, F Escourbiac, T Hirai, S Panayotis, RA Pitts, Y Corre, R Dejarnac, M Firdaouss, M Kočan, et al. Surface heat loads on the ITER divertor vertical targets. *Nuclear Fusion*, 57(4):046025, 2017.
- [3] G De Temmerman, MA Van Den Berg, J Scholten, A Lof, HJ Van Der Meiden, HJN Van Eck, TW Morgan, TM De Kruijf, PA Zeijlmans Van Emmichoven, and JJ Zielinski. High heat flux capabilities of the Magnum-PSI linear plasma device. *Fusion Engineering and Design*, 88(6-8):483–487, 2013.
- [4] H.J.N. van Eck, G.R.A. Akkermans, S. Alonso van der Westen, D.U.B. Aussems, M. van Berkel, S. Brons, I.G.J. Classen, H.J. van der Meiden, T.W. Morgan, M.J. van de Pol, J. Scholten, J.W.M. Vernimmen, E.G.P. Vos, and M.R. de Baar. High-fluence and high-flux performance characteristics of the superconducting Magnum-PSI linear plasma facility. *Fusion Engineering and Design*, 142:26–32, 2019.
- [5] GJ Van Rooij, HJ Van der Meiden, WR Koppers, AE Shumack, WAJ Vijvers, J Westerhout, GM Wright, J Rapp, et al. Thomson scattering at pilot-psi and magnum-psi. *Plasma Physics and Controlled Fusion*, 51(12):124037, 2009.
- [6] MJ van de Pol, S Alonso van der Westen, DUB Aussems, MA van den Berg, S Brons, HJN van Eck, GG van Eden, HJW Genuit, HJ van der Meiden, TW Morgan, et al. Operational characteristics of the superconducting high flux plasma generator Magnum-PSI. *Fusion Engineering and Design*, 136:597–601, 2018.
- [7] Ray Chandra, HJ De Blank, P Diomede, HJN Van Eck, HJ Van Der Meiden, TW Morgan, JWM Vernimmen, and Egbert Westerhof. B2. 5-eunomia simulations of Magnum-PSI detachment experiments: I. quantitative comparisons with experimental measurements. *Plasma Physics and Controlled Fusion*, 63(9):095006, 2021.
- [8] Sven Wiesen, Detlev Reiter, Vladislav Kotov, Martine Baelmans, Wouter Dekeyser, AS Kukushkin, SW Lisgo, RA Pitts, Vladimir Rozhansky, Gabriella Saibene, et al. The new SOLPS-ITER code package. *Journal of nuclear materials*, 463:480–484, 2015.
- [9] Detlev Reiter, Martine Baelmans, and Petra Boerner. The EIRENE and B2-EIRENE codes. *Fusion science and technology*, 47(2):172–186, 2005.
- [10] RC Wieggers, DP Coster, PWC Groen, HJ De Blank, and WJ Goedheer. B2. 5-eunomia simulations of Pilot-PSI plasmas. *Journal of Nuclear Materials*, 438:S643–S646, 2013.

- [11] D Reiter. Randschicht-konfiguration von tokamaks: Entwicklung und anwendung stochastischer modelle zur beschreibung des neutralgastransports. Technical report, 1984.
- [12] Dmitriy V Borodin, Friedrich Schluck, Sven Wiesen, DM Harting, Petra Boerner, Sebastijan Brezinsek, Wouter Dekeyser, Stefano Carli, Maarten Blommaert, Wim Van Uytven, et al. Fluid, kinetic and hybrid approaches for neutral and trace ion edge transport modelling in fusion devices. *Nuclear Fusion*, 2021.
- [13] Margarita Baeva, WJ Goedheer, NJ Lopes Cardozo, and D Reiter. B2-eirene simulation of plasma and neutrals in magnum-psi. *Journal of nuclear materials*, 363:330–334, 2007.
- [14] Juergen Rapp, Larry W Owen, John Canik, Jeremy D Lore, Juan F Caneses, Nischal Kafle, H Ray, and M Showers. Radial transport modeling of high density deuterium plasmas in proto-mpex with the b2. 5-eirene code. *Physics of Plasmas*, 26(4):042513, 2019.
- [15] Michele Sala, Elena Tonello, Andrea Uccello, Xavier Bonnin, Daria Ricci, David Dellasega, Gustavo Granucci, and Matteo Passoni. Simulations of argon plasmas in the linear plasma device gym with the solps-iter code. *Plasma Physics and Controlled Fusion*, 62(5):055005, 2020.
- [16] Ray Chandra, Hugo J de Blank, Paola Diomedea, and Egbert Westerhof. B2. 5-eunomia simulations of Magnum-PSI detachment experiments: II. collisional processes and their relevance. *Plasma Physics and Controlled Fusion*, 2021.
- [17] Ursel Fantz, D Reiter, Bernd Heger, and D Coster. Hydrogen molecules in the divertor of ASDEX upgrade. *Journal of Nuclear Materials*, 290:367–373, 2001.
- [18] Robert EH Clark. *Nuclear fusion research: understanding plasma-surface interactions*, volume 78. Springer Science & Business Media, 2005.
- [19] P Bachmann and D Reiter. Kinetic description of elastic processes in hydrogen-helium plasmas. *Contributions to Plasma Physics*, 35(1):45–100, 1995.
- [20] RC Wieggers, DP Coster, PWC Groen, HJ de Blank, and WJ Goedheer. B2. 5-eunomia simulations of pilot-psi and magnum-psi plasmas. In *20th International Conference on Plasma Surface Interactions 2012 (PSI 20)*. Citeseer.
- [21] D Tskhakaya and S Kuhn. Particle simulations of the magnetized hydrogen plasma-wall transition taking into account collisions with hydrogen atoms. In *29th EPS Conference on Controlled Fusion and Plasma Physics*, volume 26B, pages P–2.094, 2002.
- [22] D Tskhakaya, S Kuhn, Y Tomita, K Matyash, R Schneider, and F Taccogna. Self-consistent simulations of the plasma-wall transition layer. *Contributions to Plasma Physics*, 48(1-3):121–125, 2008.